Molecular Therapy
Methods & Clinical Development
Original Article

Correction of DMD in human iPSC-derived cardiomyocytes by base-editing-induced exon skipping

Peipei Wang,[1] Haiwen Li,[1] Mandi Zhu,[1] Rena Y. Han,[2] Shuliang Guo,[1] and Renzhi Han[1,3]

[1]Department of Surgery, Davis Heart and Lung Research Institute, Biomedical Sciences Graduate Program, Biophysics Graduate Program, The Ohio State University Wexner Medical Center, Columbus, OH 43210, USA; [2]Olentangy Liberty High School, Powell, OH 43065, USA

Duchenne muscular dystrophy (DMD) is caused by mutations in the *DMD* gene. Previously, we showed that adenine base editing (ABE) can efficiently correct a nonsense point mutation in a DMD mouse model. Here, we explored the feasibility of base-editing-mediated exon skipping as a therapeutic strategy for DMD using cardiomyocytes derived from human induced pluripotent stem cells (hiPSCs). We first generated a DMD hiPSC line with a large deletion spanning exon 48 through 54 (ΔE48–54) using CRISPR-Cas9 gene editing. Dystrophin expression was disrupted in DMD hiPSC-derived cardiomyocytes (iCMs) as examined by RT-PCR, western blot, and immunofluorescence staining. Transfection of ABE and a guide RNA (gRNA) targeting the splice acceptor led to efficient conversion of AG to GG (35.9% ± 5.7%) and enabled exon 55 skipping. Complete AG to GG conversion in a single clone restored dystrophin expression (42.5% ± 11% of wild type [WT]) in DMD iCMs. Moreover, we designed gRNAs to target the splice sites of exons 6, 7, 8, 43, 44, 46, and 53 in the mutational hotspots and demonstrated their efficiency to induce exon skipping in iCMs. These results highlight the great promise of ABE-mediated exon skipping as a promising therapeutic approach for DMD.

INTRODUCTION

Duchenne muscular dystrophy (DMD) is an X-linked genetic muscle disease afflicting approximately 1 in 3,800–6,300 live male births.[1] It is caused by mutations in the *DMD* gene, which codes for the protein dystrophin.[2] Dystrophin plays an important role in stabilizing the sarcolemma and mediating force transmission.[3] The muscle fibers from patients with DMD are abnormally vulnerable to mechanical stress because the mutated *DMD* gene fails to produce a functional dystrophin protein.[4] Muscle weakness of patients with DMD is usually noticeable starting in their early childhood, which gradually leads to life-threatening complications in the teen years.[5] The life expectancy of patients with DMD has increased owing to advances in better cardiac and respiratory care.[6,7] However, it is now seen that over 90% of patients with DMD die of heart failure in their late 20s to early 30s.[8] Thus, there is an urgent need to develop new therapeutic strategies to prevent heart failure in patients with DMD.

The *DMD* gene consists of 79 exons with mutations (such as nonsense, missense, deletion, duplication) spread throughout the entire gene.[9] The large deletion mutations (>1 exon) are the most common type in dystrophinopathy,[10] accounting for 68% of all DMD cases.[10] There are two hot spots ranging from exons 2 to 20 and exons 45 to 55. Exon-skipping therapy via antisense oligonucleotides (AONs), as exemplified by recent FDA approvals golodirsen (exon 53 skipping) and eteplirsen (exon 51 skipping),[11] has been developed to restore the disrupted reading frame of *DMD*, resulting in the production of partially functional dystrophin proteins.[12–20] It is estimated that ∼80% of deletions (∼55% of total mutations) could potentially be treated by exon-skipping therapy.[10] Although effective, the AON-based exon-skipping therapy requires repeated treatments. It is thus highly desirable to develop new therapeutic approaches to institute permanent exon skipping. Previous studies from our lab and others[21–36] have established the principle of concept for a gene-editing-based therapeutic approach for DMD. However, mounting evidence showed that CRISPR gene editing may cause unwanted large deletions, DNA rearrangement, and even chromosome loss because it relies on the creation of the dangerous double-strand DNA breaks (DSBs).[37–39]

New genome editing technologies are continuously emerging. Base editors (BEs), including cytosine BEs (CBEs) and adenine BEs (ABEs), can catalyze base conversion in genomic DNA without making DSBs.[40–42] We recently showed that ABE can efficiently correct a nonsense point mutation in a mouse model of DMD.[43] Although promising, correcting individual mutations for DMD is impractical. BEs can be directed to the canonical splice sites of exon/intron junctions to mutate the highly conserved splice acceptor (AG) or donor (GT), thereby triggering exon skipping.[44–46] Therefore, BEs can be developed as promising therapeutics to cure DMD.[47]

Received 13 December 2021; accepted 29 November 2022;
https://doi.org/10.1016/j.omtm.2022.11.010.

[3]Present address: Department of Pediatrics, Herman B Wells Center for Pediatric Research, Indiana University School of Medicine, Indianapolis, IN 46202, USA

Correspondence: Renzhi Han, PhD, Department of Surgery, Davis Heart and Lung Research Institute, The Ohio State University Wexner Medical Center, Columbus, OH 43210, USA.
E-mail: renzhi.han@osumc.edu

Recent advances in generating human induced pluripotent stem cells (hiPSCs) offer a convenient platform to study disease mechanisms and develop novel therapeutics.[47–50] Protocols for efficient differentiation of hiPSCs toward cardiomyocytes using defined, serum-free culture medium combined with small molecules have been developed,[49,51–53] which can be further assembled to form 3D beating structures. These engineered human heart tissues (EHHTs) resemble the biological characteristics and functions of adult human organs more accurately than regular 2D cultures.[54,55] In this study, we generated an isogenic DMD hiPSC line with exons 48–54 deleted (ΔE48–54) using CRISPR-Cas9 and demonstrated the restoration of dystrophin expression by ABE-mediated skipping of exon 55 in cardiomyocytes (CMs) and EHHTs derived from ΔE48–54 hiPSCs. Moreover, we designed guide RNAs (gRNAs) targeting additional exons within the mutational hotspots and demonstrated their efficiency to induce corresponding exon skipping in wild-type (WT) hiPSC-derived CMs (iCMs). This study highlights the great promise of ABE-mediated exon skipping as a promising therapeutic approach for DMD cardiomyopathy.

RESULTS

Generation of DMD hiPSC line with exon deletions using CRISPR-Cas9

To generate a human cell model of DMD, we explored the feasibility to generate DMD hiPSC lines using CRISPR gene editing. We designed a pair of gRNAs targeting introns 47 and 54 to delete a large genomic region spanning exons 48–54, as commonly seen in human patients with DMD (Figure 1A). The DMDi47gRNA_Cas9, DMDi54gRNA_Cas9, and GFP plasmids were co-transfected into a control hiPSC line (designated as WT) by electroporation and sorted into GFP+ single-cell clones (Figure 1B). The expanded single-cell clones were genotyped by genomic DNA PCR analysis. As shown in Figure 1C (right), an amplicon with an expected size of the targeted deletion was detected in one of the two individual clones (clone 1). Sanger sequencing confirmed that this amplicon carried the precise ligation of the two gRNA cleavage sites (Figure 1D). Although hiPSCs were derived from a female, the absence of an amplified band in clone 1 with WT oliognucleotides (oligos) (Figure 1C, left) and clean Sanger sequencing trace in Figure 1D indicated that this cell clone is likely homozygous for the deletion.

To examine if the CRISPR gene editing and single-cell cloning process affected the stemness of the hiPSCs, we performed immunofluorescence staining with antibodies against OCT4 and NANOG. Both WT and ΔE48–54 hiPSCs showed strong OCT4/NANOG staining (Figure 1E). We also performed the trilineage differentiation assay[56] to assess their differentiation potential. The expression of the ectoderm marker *PAX6*, the endoderm marker *SOX17*, and the mesoderm marker *CXCR4* were all significantly increased upon the directed differentiation (Figures S1A–S1C). There were no significant differences in the expression of *PAX6* or *CXCR4* between WT and ΔE48–54 hiPSC groups (Figures S1A and S1C), while the expression of *SOX17* was significantly lower in ΔE48–54 hiPSCs (Figure S1B), suggesting that the editing/selection processes may have some effect on endoderm differentiation.

Rescue of dystrophin expression in ΔE48–54 hiPSC-derived CMs by base-editing-induced exon skipping

Due to the disruption of the reading frame following deletion of exons 48 through 54, it is expected that dystrophin expression would be disrupted in CMs derived from ΔE48–54 hiPSCs, while skipping exon 55 would restore the dystrophin reading frame (Figure 2A). We hypothesized that ABE-induced mutation of the canonical splice acceptor of intron 54 from AG to GG would lead to exon 55 skipping. To test this, we designed a gRNA targeting the intron 54 and exon 55 junction with the nucleotide A of the splice acceptor located at position 5 of the spacer (Figure 2A). The gRNA and ABE8eV106W-SpCas9,[57] which was engineered to have increased on-target editing activity and reduced off-target RNA and DNA editing activity, were co-transfected into ΔE48–54 hiPSCs by electroporation. The editing efficiency in the pool population was 35.9% ± 5.7% as measured by BEAT[58] analysis of Sanger sequencing data (Figures 2B and 2C).

The parental and ΔE48–54 hiPSCs transfected with or without gRNA/ABE8eV106W-SpCas9 were differentiated to beating CMs (Videos S1, S2, and S3). As expected, RT-PCR analysis showed that the dystrophin transcript amplicon in CMs derived from ΔE48–54 hiPSCs was smaller compared with the parental iCMs (Figure 2D) due to the deletion of exons 48 through 54. Sanger sequencing confirmed that the amplicon from ΔE48–54-derived CMs was the product spliced from exon 47 to 55, while the smaller product from the base-edited ΔE48–54-derived CMs was due to exon 55 skipping (Figure 2E). We further sorted the gRNA/ABE8eV106W-SpCas9-P2A-EGFP transfected ΔE48–54 hiPSCs into single-cell clones. Upon differentiation into CMs, three out of the four single-cell clones (clones 2, 3, and 4) showed exon 55-skipped RT-PCR products (Figures S2 and 2D). Clone 4 was used for further studies.

Western blotting analysis showed that dystrophin was expressed in WT but not ΔE48–54 iCMs (Figure 3A). Dystrophin expression was rescued in the ΔE48–54 iCMs after gRNA/ABE8e-SpCas9NG transfection (Figures 3A and 3B) and in the CMs derived from clone 4 (Figure 3C), in which dystrophin was expressed at 42.5% ± 11% of the WT level (Figures 3A and 3B).

The iCMs were used to manufacture the EHHTs following the previously established protocol.[50,53] Immunofluorescence staining of EHHTs derived from the hiPSCs showed extensive cardiac troponin T-positive CMs in all constructs (Figure S3). Dystrophin was readily detectable in the WT and clone 4-derived EHHTs but not in ΔE48–54 EHHTs (Figure S3).

The off-target activities are one of the major concerns with gene editing therapy.[59] ABE can tolerate mismatches between the gRNA and its target sites, especially 1–2 mismatches at positions distal to the PAM.[60] We used Cas-OFFinder[61] to predict potential off-target sites, which showed that one site on chromosome 17 (Chr17_OT) has two mismatches and 20 sites have three mismatches (Figure 4A). We tested the Chr17_OT and 3 sites (Chr2_OT, Chr8_OT, Chr18_OT) with three mismatches (Figure 4B). As shown in Figure 4C, we did

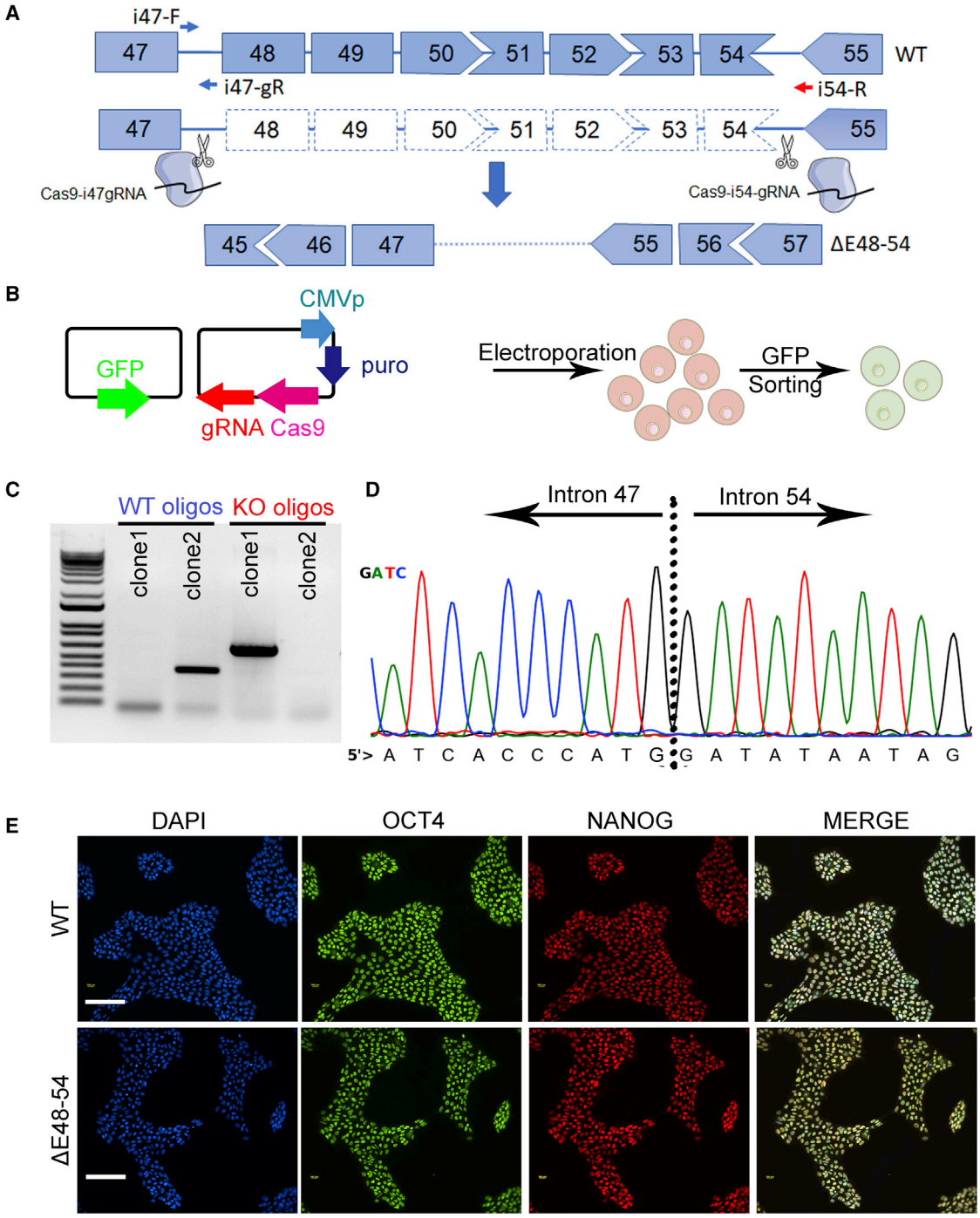

Figure 1. Establishment of DMD hiPSC line

(A) Schematic showing the targeting strategy to generate DMD hiPSCs with exon 48–54 deletion. Blue arrows indicate the location of WT oligos (i47-F and i47-R), and the red arrow shows the reverse KO oligo (i54R). The KO PCR uses the same forward oligo as for the WT PCR. (B) The transfection and screening process. (C) Genomic DNA PCR screening of two hiPSC clones with a pair of WT and KO oligos, respectively. (D) Sanger sequencing of the PCR product with the KO oligo pair. (E) Immunofluorescence staining of hiPSCs with DAPI and antibodies against OCT4 (green) and NANOG (red). Scale bar: 200 μm.

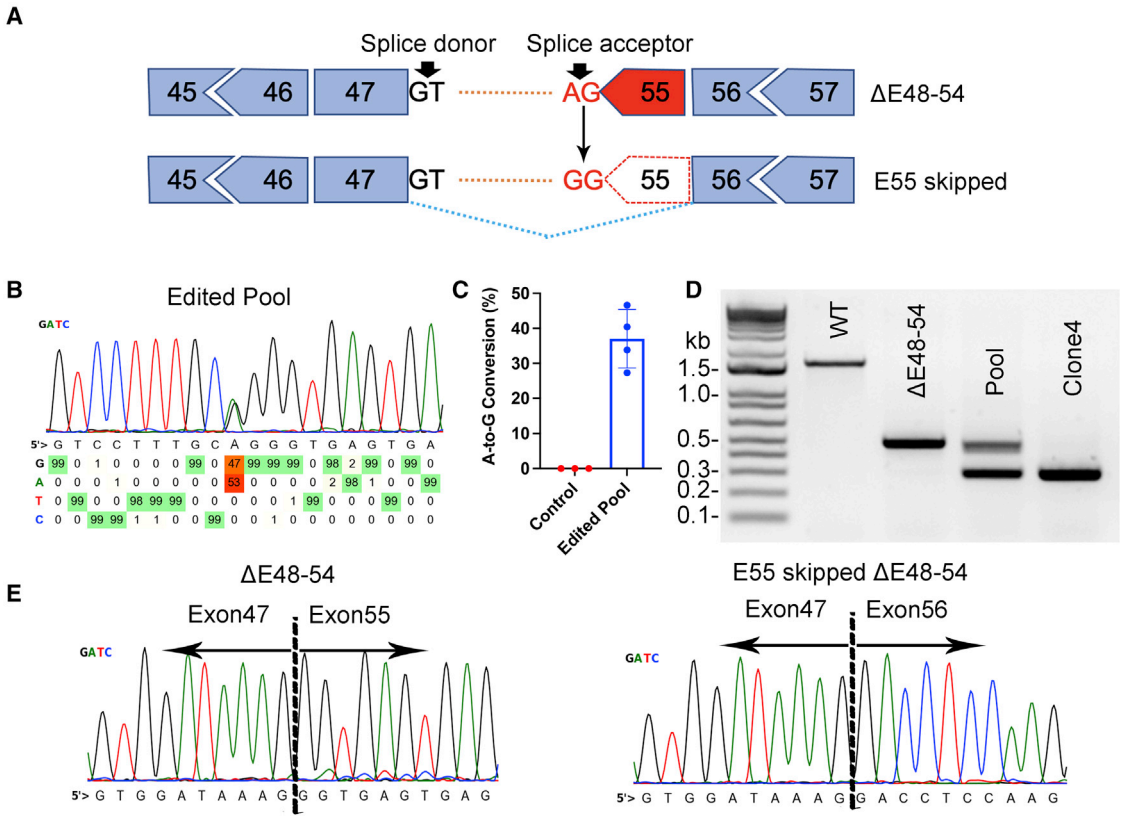

Figure 2. ABE-induced exon 55 skipping in ΔE48–54 iCMs

(A) Schematic showing the targeting strategy to induce exon 55 skipping by ABE. (B) Sanger sequencing of genomic DNA of ABE-gRNA electroporated ΔE48–54 hiPSCs. (C) Editing efficiency of ABE-gRNA electroporated ΔE48–54 hiPSCs. (D) RT-PCR analysis the dystrophin transcript amplicons in WT and ΔE48–54 iCMs with or without base editing. (E) Sanger sequencing of the RT-PCR dystrophin transcript amplicon in ΔE48–54 iCMs with or without base editing.

not observe significant editing at Chr8_OT, Chr17_OT, and Chr18_OT, but we observed 24.5% ± 0.9% editing at Chr2_OT, which is located at the donor splice site of *COBLL1* exon 1. In addition, it has been shown that ABE8e induces high bystander off-target editing.[43,47] There was only one A (at position 5) from position 1 through 10 along the spacer sequence of the exon 55 gRNA (Figure 4B), preventing us from assessing the bystander activity at the optimal editing window. The bystander editing at A11, A15, and A19 was not significant (Figure 4D).

Base-editing-induced skipping of additional exons within the mutational hotspots

After demonstration of efficient ABE-mediated skipping of exon 55 in ΔE48–54 iCMs, we further tested the feasibility of ABE-mediated exon-skipping strategy to target other exons of *DMD* that potentially allow skipping of the common mutant or out-of-frame exons within the mutational hotspots. We designed gRNAs targeting exons 6, 7, 8, 43, 44, 46, and 53 (Table 1). The gRNAs and ABE8eV106W-SpCas9 (targeting NGG PAM sites)[57] or ABE8eV106W-SpG (targeting NG PAM sites)[62] were co-transfected into hiPSCs by electroporation. The editing efficiency in each group was measured by BEAT[58] analysis of the Sanger sequencing data. The gRNAs targeting 44 and 53 showed a low editing efficiency (<5%), and the gRNA targeting exon 46 showed an efficiency of 17.1% ± 1% (Figure S4A), resulting in little to no detectable skipping of the corresponding exons (Figure S4B). In contrast, the gRNAs targeting exons 6, 7, 8, and 43 showed an efficiency above 25% (Figure 5A), leading to efficient skipping of the corresponding exons as detected by RT-PCR analysis (Figure 5B). Sanger sequencing confirmed that the smaller amplicons from the exon 6-, 7-, and 43-targeting gRNA transfected hiPSC-derived iCMs were the corresponding exon-skipping products (Figures 5C–5E). Interestingly, the gRNA targeting exon 8 triggered the skipping of both exons 8 and 9 (Figure 5F). Finally, the bystander off-target editing activities were detected for many of these gRNAs, as expected (Figure S5).

DISCUSSION

We recently demonstrated that ABE reversed a nonsense mutation with high efficiency in the heart of a mouse model of DMD. In this study, we reported the generation of a DMD hiPSC line with deletion of exons 48–54 using CRISPR-Cas9 and their differentiation into beating CMs to model DMD cardiomyopathy. We demonstrated

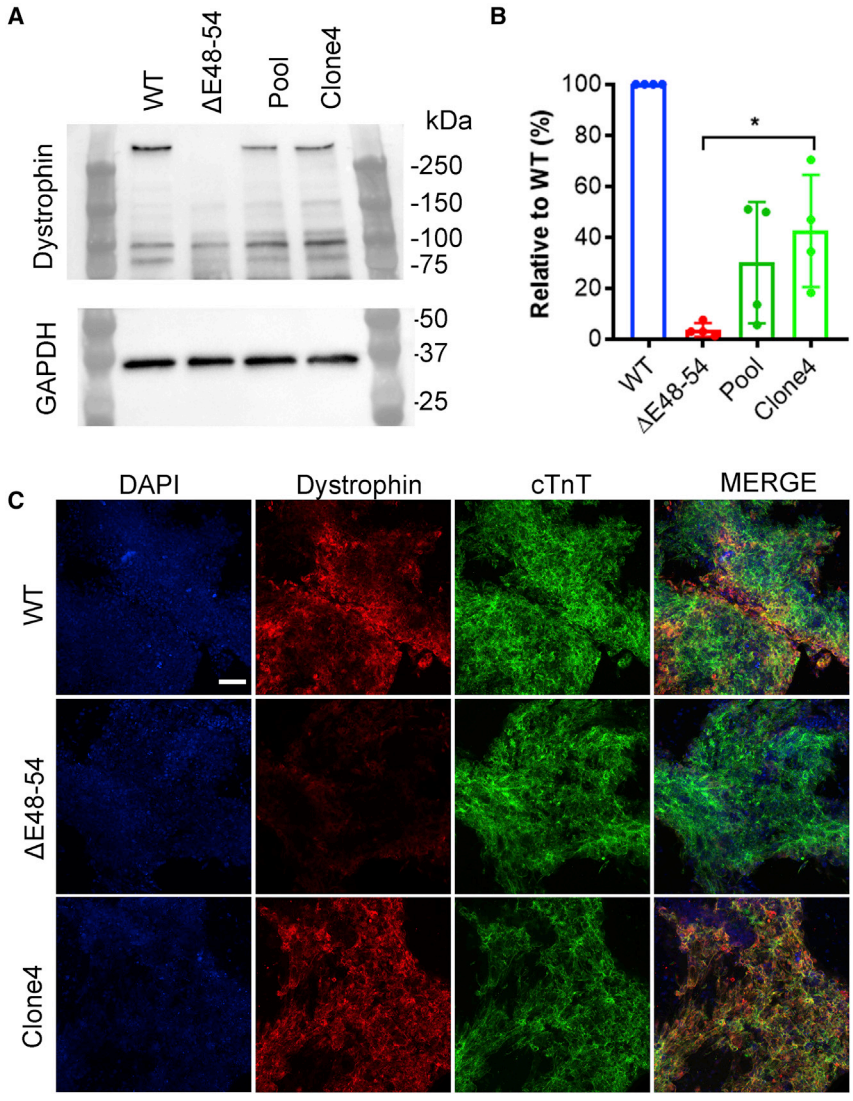

Figure 3. Rescue of dystrophin expression in ΔE48–54 iCMs by ABE-induced exon skipping

(A) Representative western blot showing the dystrophin expression in WT iCMs and ΔE48–54 iCMs with or without ABE-gRNA transfection. GAPDH was used as a loading control. (B) Densitometry quantification of the western blot data. *$p < 0.05$. (C) Immunofluorescence staining of iCMs derived from WT, ΔE48–54 hiPSCs, and clone 4 with antibodies against cardiac troponin T (cTnT) and dystrophin. Scale bars: 50 μm.

the restoration of dystrophin expression by ABE-mediated skipping of exon 55 in iCMs derived from ΔE48–54. Furthermore, we showed that the ABE-mediated exon-skipping strategy can be applied to skip other exons of *DMD* within the mutational hotspots, such as exons 6, 7, 8, and 43. Consistent with previous reports,[44,45,47] our study highlights ABE as a promising therapeutic platform to induce therapeutic exon skipping while avoiding the introduction of deleterious DSBs in genomic DNA.

Exon skipping has been achieved by ASOs,[63,64] CRISPR-Cas9,[21–36] and BEs.[44,45,47,65] Despite recent FDA approvals of several ASOs for DMD, the requirement of repeated administrations represents a major disadvantage of ASO therapy. In animal models, several groups including us showed that CRISPR-Cas9-mediated exon deletion can be efficient to restore dystrophin reading frame.[21–36] However, this CRISPR-Cas9-deletion approach is associated with a p53-dependent DNA damage response due to the creation of DSBs.[66,67] Moreover, the Cas9 nucleases can potentially lead to large genomic DNA deletions and chromosome rearrangements, as well as increased AAV integration at the Cas9 cleavage sites.[37–39] In contrast, base editing installs permanent corrections with high efficiencies, particularly in the heart,[43,68] without creating excessive DSBs, thus largely curtailing the genotoxicity of Cas9 nucleases. Compared with CBEs, ABEs offer additional advantages. First, the targeting fidelity of ABEs appears to be higher than CBEs.[65] Second, all current CBEs need the fusion of a monomeric or tandem dimeric Uracil glycosylase inhibitor (UGI) in addition to the cytosine deaminase domain, while UGI is not required for ABEs. This additional UGI domain does not only increase the size of the CBE coding sequences but also inhibits the normal function of uracil-DNA glycosylases essential for the base-excision repair pathway. The impact of long-term UGI expression from the adeno-associated virus (AAV)-delivered CBEs has not been fully explored.

Recently, Chemello et al. published an elegant study showing a similar ABE-mediated exon-skipping strategy to restore dystrophin expression in a mouse model and hiPSC-derived CMs.[47] The editing efficiency to mutate the splice donor site of exon 50 with ABEmax-SpCas9 was about 38% in HEK293T cells without sorting, which is comparable to what we observed for exon 55 splice acceptor editing in the pool population of hiPSCs after electroporation (35.9% ± 5.7%). In fluorescence-enriched, male-derived hiPSCs, the authors reported an 87.7% ± 4.1% editing efficiency, which led to a high level of dystrophin protein restoration. However, as there was no description about the editing efficiency in the pool population of hiPSCs without sorting and enrichment in that study, we could not make a direct comparison with ours. Moreover, there was no quantification of the dystrophin protein rescue in exon 51-corrected cells by western blot. It would be interesting in the future to compare the protein rescue levels following ABE-mediated skipping of different exons, which may shed light on the contributions of

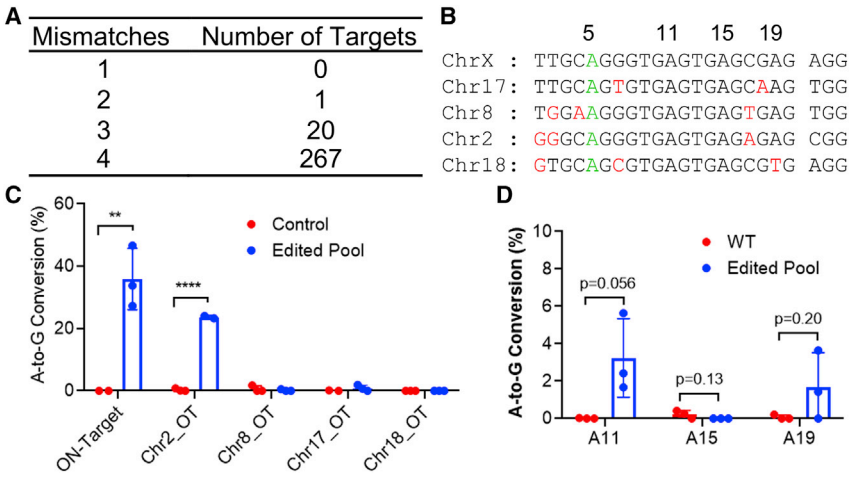

Figure 4. Off-target studies of ΔE48–54 iCMs with ABE-gRNA transfection

(A) Predicted off-target sites with a different number of mismatches from the exon 55-skipping gRNA. (B) The sequences of 4 most similar off-target sites located on chromosomes 2, 8, 17, and 18, respectively. The numbers indicate the positions of the adenines. The targeted A5 is labeled green, and mismatches are labeled red. (C) Quantification of Sanger sequencing reads of the genomic DNA PCR amplicons at the on- and off-target sites. **p < 0.01, ****p < 0.0001. (D) Quantification of the bystander editing at the on-target site.

different exon deletions to the truncated dystrophin protein stability.

In the present study, Western blot analysis showed that dystrophin was restored to only about 40% of WT levels in clone 4, which carries a 100% exon 55 skipped allele, while our previous *in vivo* studies with AAV9-delivered ABEs in *mdx*^{4cv} mice showed an efficiency higher than 85% (at transcript level) with 95% dystrophin-positive CMs.[43] Several reasons may explain why dystrophin was expressed at below WT level in iCMs. First, the truncated dystrophin protein may be less stable compared with the full-length WT dystrophin. Second, even in a pure single colony where all bases are edited, it is possible that alternative splicing may still occur with downstream cryptic splicing acceptor(s) in intron 55 to produce large intron retention products, for which RT-PCR may not detect due to the large size or nonsense-mediated decay. Third, the differentiation and maturation status of iPSCs varied among different clones and different experiments.[69] Finally, the electroporation and single-cell colony screening process may further have detrimental effects on their differentiation/maturation status, thus reducing the expression of cardiac-related genes. Nevertheless, 40% dystrophin rescue should still have clinical benefits, as previous research showed that 10%–20% of dystrophin was functionally protective.[70,71]

Although animal models are valuable for proof-of-principle studies, gene editing therapeutics are highly sequence and context dependent, thus requiring suitable human models for preclinical development. The advancements in hiPSC reprogramming, differentiation, and 3D micro-tissue manufacturing offer an unprecedented research platform for disease pathogenesis and therapeutic development studies that are directly relevant to a human genomic context. We generated a DMD-hiPSC line with a large deletion from exons 48 to 54 using CRISPR-Cas9 gene editing and their differentiation to beating CMs. This platform would greatly facilitate the preclinical development of gene editing therapeutics for human diseases. In addition, the gene-corrected hiPSCs and their derived myocytes could provide a renewable resource of cells for transplantation therapy if breakthroughs were made to improve the *in vivo* grafting, differentiation, and maturation efficiency in the future. Compared with the *in vivo* gene editing therapy via viral (AAV) or non-viral (such as lipid nanoparticles) delivery approaches, cell transplantation therapy has the advantage of potentially avoiding the genotoxicity associated with the delivery vehicles and gene editing reagents. Off-target editing could be minimized and/or eliminated before transplantation. Indeed, transplantation of hiPSC-derived CMs has shown great promise in regenerating injured heart tissues *in vivo*.[72–75] The engrafted hiPSC-derived CMs can make physiological connections with the host CMs and promote recovery of host myocardium. However, low grafting efficiency, potential tumorigenicity, immune rejection, and graft-associated arrhythmia are major concerns about this therapeutic strategy[75] and warrant intensive future investigations.

MATERIALS AND METHODS

Plasmid construction

The ABE plasmids including ABE8e(TadA-8eV106W)-nSpCas9 (Addgene #138495),[57] pCMV-T7-ABEmax_7.10-SpG-P2A-EGFP_RTW4562 (Addgene #140002),[62] and pCMV-ABEmax (Addgene #112095)[76] were obtained from Addgene (Watertown, MA, USA). pLKO-puro-E2A-GFP plasmid was described previously.[77] ABE8eV106W-SpG-P2A-EGFP was constructed by PCR of the ABE8eV106W from ABE8e(TadA-8eV106W)-nSpCas9 and inserted into the NotI/BglII of pCMV-T7-ABEmax_7.10-SpG-P2A-EGFP_RTW4562. ABE8eV106W-nSpCas9-P2A-EGFP was constructed by amplifying the nSpCas9 from ABE8e(TadA-8eV106W)-nSpCas9 and inserted into PspOMI/EcoRI of ABE8eV106W-SpG-P2A-EGFP. The gRNAs were designed to target the human *DMD* gene. The annealed gRNA oligos were cloned into pLenti-OgRNA-Zeo[43] or pLKO-ogRNA-puro2A-hCas9 plasmids.[77] All oligos for gRNAs and PCR are listed in Table S1. All plasmids are listed in Table S2.

Cell culture

Human iPSCs were purchased from Thermo Fisher Scientific (cat. #A18945, Waltham, MA, USA). They were grown on Matrigel (Corning #356231, NY, USA) coated 6-well plates and maintained in Essential 8 Flex Medium (Gibco, Thermo Fisher Scientific) at 37°C with 95% air and 5% CO_2. Cells were passaged at 70%–80% confluence using TrypLE Express Enzyme (Gibco).

Table 1. Guide RNA targets of the splice site for exon skipping

Exon	SD/SA	Sequence	PAM	ABE used
6	SD	ttcttacCTATGACTATGGA	TGA	ABE106W-SpG
7	SD	accaacCTTCAGGATCGAGT	AGT	ABE106W-SpG
8	SD	actttacCTGTTGAGAATAG	TGC	ABE106W-SpG
43	SD	tacctacCCTTGTCGGTCCT	TGT	ABE106W-SpG
44	SA	tgcagGCGATTTGACAGATC	TGT	ABE106W-SpG
46	SA	ctccagGCTAGAAGAACAAA	AGA	ABE106W-SpG
53	SA	tattctagTTGAAAGAATTC	AGA	ABE106W-SpG
55	SA	ttgcagGGTGAGTGAGCGAG	AGG	ABE106W-SpCas9

Human cardiac ventricular fibroblasts (HCVFBs) were purchased from Lonza (#CC-2904, Bend, OR, USA) and cultured in FGM-2 medium (CC-3132, Lonza). Human adipose-derived stem cells (hADSCs) were purchased from Lonza (#PT5006) and cultured in low-glucose Dulbecco's modified Eagle's medium supplemented with 10% fetal bovine serum (FBS; Gibco) and 1% penicillin-streptomycin, 1% glutamine, and 1% antimycin (Gibco). Human umbilical vein endothelial cells (HUVECs) were purchased from Lonza (cat. #C2519A) and cultured in EGM-3 medium (Lonza). HCVFBs, hADSCs, and HUVECs were used at passages of 3–5 after purchasing for cardiac organoid fabrication.

Electroporation and selection of hiPSCs

hiPSCs were dissociated into single cells using TrypLE Express Enzyme. To generate ΔE48–54 cell line, 1×10^6 hiPSCs were mixed with 5 μg gRNA-hCas9 plasmid and 0.5 μg GFP plasmid. For the base editing studies, 1×10^6 cells were mixed with 2.5 μg ABE, 2.5 μg gRNA, and 0.5 μg GFP plasmid. The cell-plasmid mixtures were electroporated using the Neon transfection system (Thermo Fisher Scientific) with the conditions of 1,200 V, 30 ms, and 1 pulse. The day following transfection, cells were treated with 1 μg/mL puromycin in Essential 8 medium for 24 h to enrich transfected cells. The cells were cultured for 3 more days in Essential 8 medium then either differentiated into CMs or sorted into individual 96-well plate to generate single-cell clones using Aria III at the Analytical Cytometry Shared Resource of the Ohio State University Comprehensive Cancer Center. After 10 to 14 days, individual colonies were passaged and screened by PCR analysis.

CM differentiation of hiPSCs

hiPSCs were differentiated into CMs as described by Zhao et al.[49] Briefly, cells were trypsinized with TrypLE Express Enzyme and plated as single cells on Matrigel-coated 6-well plates in Essential 8 Medium. When the cells reached 70%–80% confluency, they were cultured in RPMI 1640 medium supplemented with B-27 minus insulin (Gibco) and 8 μM CHIR-99021 (Selleckchem, Houston, TX, USA) (days 1–2). After 2 days, the medium was changed to RPMI 1640 medium supplemented with B-27 minus insulin for 1 day (day 3), followed by RPMI 1640 medium supplemented with B-27 minus insulin and 5 μM IWR-1 (Sigma, St. Louis, MO, USA) for 2 days (days 4–5). The medium was replaced with RPMI 1640 medium supplemented with B-27 minus insulin for another 2 days (days 6–7) and substituted with cardiac proliferation medium, which is RPMI 1640 medium supplemented with B-27 (Gibco), for 2 days (days 8–9). Then, the differentiated cells were selected with the media RPMI 1640 without glucose (Gibco) supplemented with B-27 for 4 days (days 10–13) and then cardiac proliferation medium thereafter. CMs were used for experiments between days 20 and 30.

EHHTs

Human iPSC-CMs, HCVFBs, hADSCs, and HUVECs were constructed into EHHTs as adapted from Richards et al.[50] Briefly, agarose hydrogel molds were generated from the MicroTissues 3D Petri Dish (Z764051, Sigma) according to the manufacturer's protocol and transferred to 24-well plates. Cell suspensions with 50% hiPSC-CMs and 50% non-myocyte (including FBs, HUVECs, and hADSCs at a 4:2:1 ratio) were prepared in culture medium (F12/DMEM with 10% FBS, 1% glutamine, and 1% non-essential amino acids) (Gibco) at a final concentration of 2×10^6 cells/mL, and then 75 μL of the cell suspension was pipetted into each agarose mold and incubated at 37°C for 15 min to let the cells settle into the recesses of the mold. One mL culture medium was then added to submerge the molds and exchanged every 2 days for a total of 10 days.

PCR and Sanger sequencing

Genomic DNA or total RNA was extracted from hiPSCs or iCMs. PCR reactions were carried out with 100 ng genomic DNA or cDNA in the GoTaq Master Mix (Promega) according to the manufacturer's instruction. PCR conditions were 5 min at 95°C, followed by 32 cycles of 30 s at 95°C, 30 s at 60°C, and 30 s at 72°C. The PCR products were run on a 1% or 3% agarose gel and purified using the Wizard SV Gel and PCR Clean-up System (Promega). Purified PCR products (100 ng) were subjected to Sanger sequencing at the Genomics Shared Resource of the Ohio State University Comprehensive Cancer Center and analyzed by BEAT program.[58]

Trilineage differentiation assay

WT and ΔE48–54 hiPSC lines underwent *in-vitro*-directed differentiation using the STEMdiff Trilineage Differentiation Kit (StemCell Technologies, cat. #05230) according to manufacturer's instruction. Briefly, hiPSCs were seeded onto 12-well plates coated with Matigel at 400,000 cells/well for both the ectoderm and endoderm differentiation and 100,000 cells/well for the mesoderm differentiation and treated with the appropriate differentiation media. Differentiated cells were then collected for RNA isolation for quantitative real-time RT-PCR.

Quantitative real-time RT-PCR

RNA was isolated using Quick-RNA MiniPrep Kit (ZYMO Research, Irvine, CA, USA). 100 ng RNA was used as template for first-strand cDNA synthesis using RevertAid RT Reverse Transcription Kit (Life Technologies, Carlsbad, CA, USA) according to manufacturer's instruction. Real-time PCR was performed using PowerUp SYBR Green Master Mix (Applied Biosystems, Thermo Fisher Scientific)

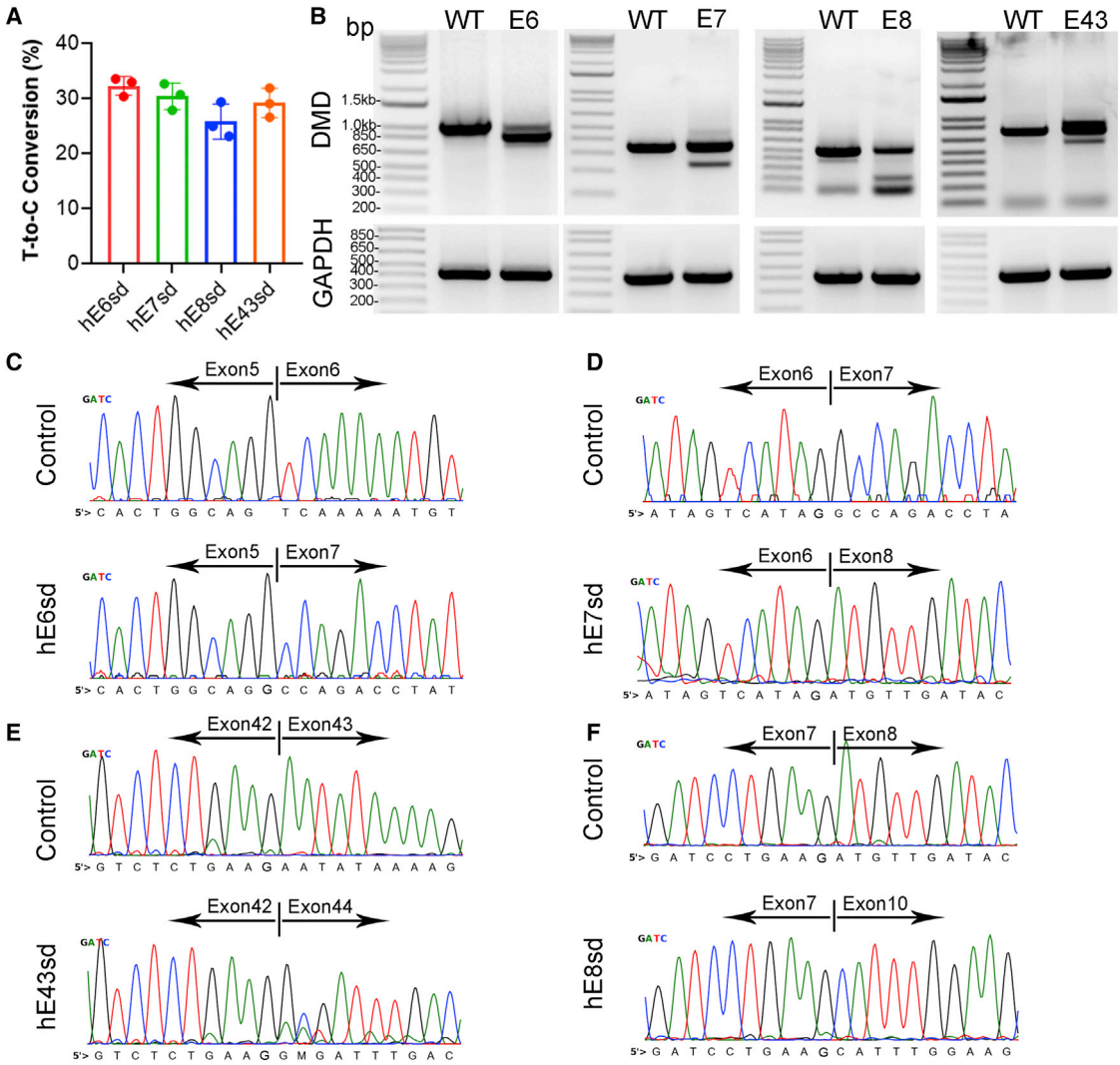

Figure 5. Exon 6, 7, 8, and 43 skipping induced by ABE

(A) BEAT quantification of the editing efficiency at splice donor sites in iCMs transfected with ABE and the corresponding targeting gRNAs. (B) RT-PCR analysis of the dystrophin transcript amplicons in iCMs transfected with or without ABE and the corresponding targeting gRNAs. (C–F) Sanger sequencing of the WT and smaller dystrophin transcript amplicons shown in (B).

in CFX384 Real-time PCR Detection Systems (Bio-Rad, Hercules, CA, USA). Samples were normalized for expression of GAPDH and analyzed by the $2^{-\Delta\Delta Ct}$ method.

Western blot analysis

Cells in each group were lysed with cold radioimmunoprecipitation assay (RIPA) buffer supplemented with protease inhibitors, and extracted protein samples were separated by SDS-PAGE (Bio-Rad, 4%–15%) and transferred onto Nitrocellulose membranes (0.45 μm). The mouse monoclonal anti-dystrophin (MANDRA1, cat. #MA1-26837 1:1,000, Invitrogen, Carlsbad, CA, USA) and rabbit monoclonal anti-Gapdh (2118 S, 14C10, 1:2,000, Cell Signaling Technology, Danvers, MA, USA) antibodies were used for immunoblotting analysis. Horseradish peroxide (HRP)-conjugated goat anti-mouse (7076 S, 1:2,000) and goat anti-rabbit (7074 S, 1:2,000) secondary antibodies were obtained from Cell Signaling Technology. The membranes were developed using enhanced chemiluminescence (ECL) western blotting substrate (Pierce Biotechnology, Rockford, IL, USA) and scanned by ChemiDoc XRS+ system (Bio-Rad). Western blots were quantified using Image Lab 6.0.1 software (Bio-Rad) according to the manufacturer's instruction.

Immunofluorescence analysis

EHHTs with mold were embedded in optimal cutting temperature (OCT) compound (Sakura Finetek, Alphen aan den Rijn, the Netherlands), snap frozen in cold isopentane, and stored at −80°C.

Frozen cryosections (7 μm), hiPSCs, or iCMs on glass coverslips were fixed with 4% paraformaldehyde for 10 min at room temperature. After washing with phosphate-buffered saline (PBS), the slides and glass coverslips were blocked with 4% BSA with 0.15% Triton X-100 at room temperature for 1 h. The slides and glass coverslips were incubated with primary antibodies including dystrophin (MANDRA1, 1:200), cardiac troponin T (cTnT; ab209813, 1:200, Abcam), OCT4 (PA5-27438, 1:300, Invitrogen), or NANOG (PA1-097, 1:200, Invitrogen) at 4°C overnight. After that, the slides and glass coverslips were warmed up at room temperature for 30 min, washed with PBS and incubated with secondary antibodies Alexa Fluor 555 goat anti-mouse IgG (1:400, Invitrogen) or Alexa Fluor 488 donkey anti-rabbit IgG (1:400, Invitrogen) for 1 h at room temperature. The slides and glass coverslips were sealed with VECTASHIELD Antifade Mounting Medium with DAPI (Vector Laboratory, Burlingame, CA, USA). All images were taken under a Nikon Ti-E fluorescence microscope (magnification 200×).

Statistics

The data are expressed as the mean ± SEM. Statistical significance was determined using Student's t test for two groups or one-way ANOVA analysis followed by Bonferroni post hoc tests for multiple groups using GraphPad Prism 8 (GraphPad Software, La Jolla, CA, USA). A p value <0.05 was considered significant.

DATA AVAILABILITY

All relevant data supporting the key findings of this study are available within the article and its supplemental information files or from the corresponding author upon reasonable request.

SUPPLEMENTAL INFORMATION

Supplemental information can be found online at https://doi.org/10.1016/j.omtm.2022.11.010.

ACKNOWLEDGMENTS

We thank members of the Han lab for helpful discussion and suggestions. R.H. is supported US National Institutes of Health grants (R01HL116546 and R01HL159900), a Parent Project Muscular Dystrophy award, and the Miao Family gift. R.H. has received industry research support (unrelated to this study) from Stealth Biotherapeutics.

AUTHOR CONTRIBUTIONS

R.H. conceived the study and revised the manuscript. P.W. performed the experiments, analyzed the data, and drafted the initial manuscript. H.L. performed confocal imaging, and S.G. assisted in plasmid construction. M.Z. and R.Y.H. performed genomic DNA extraction and PCR. All co-authors have reviewed and approved the final version of the manuscript prior to submission.

DECLARATION OF INTERESTS

A patent related to this work has been filed.

REFERENCES

1. Landfeldt, E., Thompson, R., Sejersen, T., McMillan, H.J., Kirschner, J., and Lochmüller, H. (2020). Life expectancy at birth in Duchenne muscular dystrophy: a systematic review and meta-analysis. Eur. J. Epidemiol. *35*, 643–653.
2. Forrest, S.M., Cross, G.S., Flint, T., Speer, A., Robson, K.J., and Davies, K.E. (1988). Further studies of gene deletions that cause Duchenne and Becker muscular dystrophies. Genomics *2*, 109–114.
3. Bonilla, E., Samitt, C.E., Miranda, A.F., Hays, A.P., Salviati, G., DiMauro, S., Kunkel, L.M., Hoffman, E.P., and Rowland, L.P. (1988). Duchenne muscular dystrophy: deficiency of dystrophin at the muscle cell surface. Cell *54*, 447–452.
4. Aartsma-Rus, A., Ginjaar, I.B., and Bushby, K. (2016). The importance of genetic diagnosis for Duchenne muscular dystrophy. J. Med. Genet. *53*, 145–151.
5. Deconinck, N., and Dan, B. (2007). Pathophysiology of duchenne muscular dystrophy: current hypotheses. Pediatr. Neurol. *36*, 1–7.
6. Ishikawa, Y., Miura, T., Ishikawa, Y., Aoyagi, T., Ogata, H., Hamada, S., and Minami, R. (2011). Duchenne muscular dystrophy: survival by cardio-respiratory interventions. Neuromuscul. Disord. *21*, 47–51.
7. Sheehan, D.W., Birnkrant, D.J., Benditt, J.O., Eagle, M., Finder, J.D., Kissel, J., Kravitz, R.M., Sawnani, H., Shell, R., Sussman, M.D., and Wolfe, L.F. (2018). Respiratory management of the patient with Duchenne muscular dystrophy. Pediatrics *142*, S62–S71.
8. Fayssoil, A., Nardi, O., Orlikowski, D., and Annane, D. (2010). Cardiomyopathy in Duchenne muscular dystrophy: pathogenesis and therapeutics. Heart Fail. Rev. *15*, 103–107.
9. Echigoya, Y., Lim, K.R.Q., Nakamura, A., and Yokota, T. (2018). Multiple exon skipping in the duchenne muscular dystrophy hot spots: prospects and challenges. J. Pers. Med. *8*, 41.
10. Bladen, C.L., Salgado, D., Monges, S., Foncuberta, M.E., Kekou, K., Kosma, K., Dawkins, H., Lamont, L., Roy, A.J., Chamova, T., et al. (2015). The TREAT-NMD DMD Global Database: analysis of more than 7, 000 Duchenne muscular dystrophy mutations. Hum. Mutat. *36*, 395–402.
11. Aartsma-Rus, A., and Corey, D.R. (2020). The 10th oligonucleotide therapy approved: golodirsen for duchenne muscular dystrophy. Nucleic Acid Ther. *30*, 67–70.
12. Niks, E.H., and Aartsma-Rus, A. (2017). Exon skipping: a first in class strategy for Duchenne muscular dystrophy. Expert Opin. Biol. Ther. *17*, 225–236.
13. Cirak, S., Arechavala-Gomeza, V., Guglieri, M., Feng, L., Torelli, S., Anthony, K., Abbs, S., Garralda, M.E., Bourke, J., Wells, D.J., et al. (2011). Exon skipping and dystrophin restoration in patients with Duchenne muscular dystrophy after systemic phosphorodiamidate morpholino oligomer treatment: an open-label, phase 2, dose-escalation study. Lancet *378*, 595–605.
14. Bremmer-Bout, M., Aartsma-Rus, A., De Meijer, E.J., Kaman, W.E., Janson, A.A.M., Vossen, R.H.A.M., van Ommen, G.-J.B., Den Dunnen, J.T., and van Deutekom, J.C.T. (2004). Targeted exon skipping in transgenic hDMD mice: a model for direct preclinical screening of human-specific antisense oligonucleotides. Mol. Ther. *10*, 232–240.
15. Mcclorey, G., Moulton, H.M., Iversen, P.L., Fletcher, S., and Wilton, S.D. (2006). Antisense oligonucleotide-induced exon skipping restores dystrophin expression in vitro in a canine model of DMD. Gene Ther. *13*, 1373–1381.
16. Yin, H., Lu, Q., and Wood, M. (2008). Effective exon skipping and restoration of dystrophin expression by peptide nucleic acid antisense oligonucleotides in mdx mice. Mol. Ther. *16*, 38–45.
17. Echigoya, Y., and Yokota, T. (2014). Skipping multiple exons of dystrophin transcripts using cocktail antisense oligonucleotides. Nucleic Acid Ther. *24*, 57–68.
18. Van Deutekom, J.C., Bremmer-Bout, M., Janson, A.A., Ginjaar, I.B., Baas, F., den Dunnen, J.T., and van Ommen, G.J. (2001). Antisense-induced exon skipping restores dystrophin expression in DMD patient derived muscle cells. Hum. Mol. Genet. *10*, 1547–1554.
19. Popplewell, L.J., Trollet, C., Dickson, G., and Graham, I.R. (2009). Design of phosphorodiamidate morpholino oligomers (PMOs) for the induction of exon skipping of the human DMD gene. Mol. Ther. *17*, 554–561.
20. Béroud, C., Tuffery-Giraud, S., Matsuo, M., Hamroun, D., Humbertclaude, V., Monnier, N., Moizard, M.P., Voelckel, M.A., Calemard, L.M., Boisseau, P., et al.

(2007). Multiexon skipping leading to an artificial DMD protein lacking amino acids from exons 45 through 55 could rescue up to 63% of patients with Duchenne muscular dystrophy. Hum. Mutat. *28*, 196–202.

21. Xu, L., Park, K.H., Zhao, L., Xu, J., El Refaey, M., Gao, Y., Zhu, H., Ma, J., and Han, R. (2016). CRISPR-mediated genome editing restores dystrophin expression and function in mdx mice. Mol. Ther. *24*, 564–569.

22. El Refaey, M., Xu, L., Gao, Y., Canan, B.D., Adesanya, T.M.A., Warner, S.C., Akagi, K., Symer, D.E., Mohler, P.J., Ma, J., et al. (2017). In vivo genome editing restores dystrophin expression and cardiac function in dystrophic mice. Circ. Res. *121*, 923–929.

23. Bengtsson, N.E., Hall, J.K., Odom, G.L., Phelps, M.P., Andrus, C.R., Hawkins, R.D., Hauschka, S.D., Chamberlain, J.R., and Chamberlain, J.S. (2017). Muscle-specific CRISPR/Cas9 dystrophin gene editing ameliorates pathophysiology in a mouse model for Duchenne muscular dystrophy. Nat. Commun. *8*, 14454.

24. Young, C.S., Hicks, M.R., Ermolova, N.V., Nakano, H., Jan, M., Younesi, S., Karumbayaram, S., Kumagai-Cresse, C., Wang, D., Zack, J.A., et al. (2016). A single CRISPR-cas9 deletion strategy that targets the majority of DMD patients restores dystrophin function in hiPSC-derived muscle cells. Cell Stem Cell *18*, 533–540.

25. Long, C., Amoasii, L., Mireault, A.A., McAnally, J.R., Li, H., Sanchez-Ortiz, E., Bhattacharyya, S., Shelton, J.M., Bassel-Duby, R., and Olson, E.N. (2016). Postnatal genome editing partially restores dystrophin expression in a mouse model of muscular dystrophy. Science *351*, 400–403.

26. Ousterout, D.G., Kabadi, A.M., Thakore, P.I., Majoros, W.H., Reddy, T.E., and Gersbach, C.A. (2015). Multiplex CRISPR/Cas9-based genome editing for correction of dystrophin mutations that cause Duchenne muscular dystrophy. Nat. Commun. *6*, 6244.

27. Li, H.L., Fujimoto, N., Sasakawa, N., Shirai, S., Ohkame, T., Sakuma, T., Tanaka, M., Amano, N., Watanabe, A., Sakurai, H., et al. (2015). Precise correction of the dystrophin gene in duchenne muscular dystrophy patient induced pluripotent stem cells by TALEN and CRISPR-cas9. Stem Cell Rep. *4*, 143–154.

28. Tabebordbar, M., Zhu, K., Cheng, J.K.W., Chew, W.L., Widrick, J.J., Yan, W.X., Maesner, C., Wu, E.Y., Xiao, R., Ran, F.A., et al. (2016). In vivo gene editing in dystrophic mouse muscle and muscle stem cells. Science *351*, 407–411.

29. Nelson, C.E., Hakim, C.H., Ousterout, D.G., Thakore, P.I., Moreb, E.A., Castellanos Rivera, R.M., Madhavan, S., Pan, X., Ran, F.A., Yan, W.X., et al. (2016). In vivo genome editing improves muscle function in a mouse model of Duchenne muscular dystrophy. Science *351*, 403–407.

30. Zhang, Y., Long, C., Li, H., McAnally, J.R., Baskin, K.K., Shelton, J.M., Bassel-Duby, R., and Olson, E.N. (2017). CRISPR-Cpf1 correction of muscular dystrophy mutations in human cardiomyocytes and mice. Sci. Adv. *3*, e1602814.

31. Hakim, C.H., Wasala, N.B., Nelson, C.E., Wasala, L.P., Yue, Y., Louderman, J.A., Lessa, T.B., Dai, A., Zhang, K., Jenkins, G.J., et al. (2018). AAV CRISPR editing rescues cardiac and muscle function for 18 months in dystrophic mice. JCI Insight *3*, e124297.

32. Nelson, C.E., Wu, Y., Gemberling, M.P., Oliver, M.L., Waller, M.A., Bohning, J.D., Robinson-Hamm, J.N., Bulaklak, K., Castellanos Rivera, R.M., Collier, J.H., et al. (2019). Long-term evaluation of AAV-CRISPR genome editing for Duchenne muscular dystrophy. Nat. Med. *25*, 427–432.

33. Amoasii, L., Hildyard, J.C.W., Li, H., Sanchez-Ortiz, E., Mireault, A., Caballero, D., Harron, R., Stathopoulou, T.R., Massey, C., Shelton, J.M., et al. (2018). Gene editing restores dystrophin expression in a canine model of Duchenne muscular dystrophy. Science *362*, 86–91.

34. Iyombe-Engembe, J.P., Ouellet, D.L., Barbeau, X., Rousseau, J., Chapdelaine, P., Lagüe, P., and Tremblay, J.P. (2016). Efficient restoration of the dystrophin gene reading frame and protein structure in DMD myoblasts using the CinDel method. Mol. Ther. Nucleic Acids *5*, e283.

35. Duchêne, B.L., Cherif, K., Iyombe-Engembe, J.P., Guyon, A., Rousseau, J., Ouellet, D.L., Barbeau, X., Lague, P., and Tremblay, J.P. (2018). CRISPR-induced deletion with SaCas9 restores dystrophin expression in dystrophic models in vitro and in vivo. Mol. Ther. *26*, 2604–2616.

36. Xu, L., Lau, Y.S., Gao, Y., Li, H., and Han, R. (2019). Life-long AAV-mediated CRISPR genome editing in dystrophic heart improves cardiomyopathy without causing serious lesions in mdx mice. Mol. Ther. *27*, 1407–1414.

37. Kosicki, M., Tomberg, K., and Bradley, A. (2018). Repair of double-strand breaks induced by CRISPR-Cas9 leads to large deletions and complex rearrangements. Nat. Biotechnol. *36*, 765–771.

38. Adikusuma, F., Piltz, S., Corbett, M.A., Turvey, M., McColl, S.R., Helbig, K.J., Beard, M.R., Hughes, J., Pomerantz, R.T., and Thomas, P.Q. (2018). Large deletions induced by Cas9 cleavage. Nature *560*, E8–E9.

39. Shin, H.Y., Wang, C., Lee, H.K., Yoo, K.H., Zeng, X., Kuhns, T., Yang, C.M., Mohr, T., Liu, C., and Hennighausen, L. (2017). CRISPR/Cas9 targeting events cause complex deletions and insertions at 17 sites in the mouse genome. Nat. Commun. *8*, 15464.

40. Komor, A.C., Kim, Y.B., Packer, M.S., Zuris, J.A., and Liu, D.R. (2016). Programmable editing of a target base in genomic DNA without double-stranded DNA cleavage. Nature *533*, 420–424.

41. Nishida, K., Arazoe, T., Yachie, N., Banno, S., Kakimoto, M., Tabata, M., Mochizuki, M., Miyabe, A., Araki, M., Hara, K.Y., et al. (2016). Targeted nucleotide editing using hybrid prokaryotic and vertebrate adaptive immune systems. Science *353*, aaf8729.

42. Gaudelli, N.M., Komor, A.C., Rees, H.A., Packer, M.S., Badran, A.H., Bryson, D.I., and Liu, D.R. (2017). Programmable base editing of A· T to G· C in genomic DNA without DNA cleavage. Nature *551*, 464–471.

43. Xu, L., Zhang, C., Li, H., Wang, P., Gao, Y., Mokadam, N.A., Ma, J., Arnold, W.D., and Han, R. (2021). Efficient precise in vivo base editing in adult dystrophic mice. Nat. Commun. *12*, 3719.

44. Winter, J., Luu, A., Gapinske, M., Manandhar, S., Shirguppe, S., Woods, W.S., Song, J.S., and Perez-Pinera, P. (2019). Targeted exon skipping with AAV-mediated split adenine base editors. Cell Discov. *5*, 56.

45. Gapinske, M., Luu, A., Winter, J., Woods, W.S., Kostan, K.A., Shiva, N., Song, J.S., and Perez-Pinera, P. (2018). CRISPR-SKIP: programmable gene splicing with single base editors. Genome Biol. *19*, 107.

46. Yuan, J., Ma, Y., Huang, T., Chen, Y., Peng, Y., Li, B., Li, J., Zhang, Y., Song, B., Sun, X., et al. (2018). Genetic modulation of RNA splicing with a CRISPR-guided cytidine deaminase. Mol. Cell *72*, 380–394.e7.

47. Chemello, F., Chai, A.C., Li, H., Rodriguez-Caycedo, C., Sanchez-Ortiz, E., Atmanli, A., Mireault, A.A., Liu, N., Bassel-Duby, R., and Olson, E.N. (2021). Precise correction of Duchenne muscular dystrophy exon deletion mutations by base and prime editing. Sci. Adv. *7*, eabg4910.

48. Long, C., Li, H., Tiburcy, M., Rodriguez-Caycedo, C., Kyrychenko, V., Zhou, H., Zhang, Y., Min, Y.-L., Shelton, J.M., Mammen, P.P.A., et al. (2018). Correction of diverse muscular dystrophy mutations in human engineered heart muscle by single-site genome editing. Sci. Adv. *4*, eaap9004.

49. Zhao, M.-T., Chen, H., Liu, Q., Shao, N.-Y., Sayed, N., Wo, H.-T., Zhang, J.Z., Ong, S.-G., Liu, C., Kim, Y., et al. (2017). Molecular and functional resemblance of differentiated cells derived from isogenic human iPSCs and SCNT-derived ESCs. Proc. Natl. Acad. Sci. USA *114*, E11111–E11120.

50. Richards, D.J., Li, Y., Kerr, C.M., Yao, J., Beeson, G.C., Coyle, R.C., Chen, X., Jia, J., Damon, B., Wilson, R., et al. (2020). Human cardiac organoids for the modelling of myocardial infarction and drug cardiotoxicity. Nat. Biomed. Eng. *4*, 446–462.

51. Lian, X., Zhang, J., Azarin, S.M., Zhu, K., Hazeltine, L.B., Bao, X., Hsiao, C., Kamp, T.J., and Palecek, S.P. (2013). Directed cardiomyocyte differentiation from human pluripotent stem cells by modulating Wnt/beta-catenin signaling under fully defined conditions. Nat. Protoc. *8*, 162–175.

52. Burridge, P.W., Matsa, E., Shukla, P., Lin, Z.C., Churko, J.M., Ebert, A.D., Lan, F., Diecke, S., Huber, B., Mordwinkin, N.M., et al. (2014). Chemically defined generation of human cardiomyocytes. Nat. Methods *11*, 855–860.

53. Yang, X., Pabon, L., and Murry, C.E. (2014). Engineering adolescence: maturation of human pluripotent stem cell-derived cardiomyocytes. Circ. Res. *114*, 511–523.

54. Sharma, A., Sances, S., Workman, M.J., and Svendsen, C.N. (2020). Multi-lineage human iPSC-derived platforms for disease modeling and drug discovery. Cell Stem Cell *26*, 309–329.

55. Zhao, D., Lei, W., and Hu, S. (2021). Cardiac organoid-a promising perspective of preclinical model. Stem Cell Res. Ther. *12*, 272–310.

56. Kuang, Y.L., Munoz, A., Nalula, G., Santostefano, K.E., Sanghez, V., Sanchez, G., Terada, N., Mattis, A.N., Iacovino, M., Iribarren, C., et al. (2019). Evaluation of

commonly used ectoderm markers in iPSC trilineage differentiation. Stem Cell Res. *37*, 101434.

57. Richter, M.F., Zhao, K.T., Eton, E., Lapinaite, A., Newby, G.A., Thuronyi, B.W., Wilson, C., Koblan, L.W., Zeng, J., Bauer, D.E., et al. (2020). Phage-assisted evolution of an adenine base editor with improved Cas domain compatibility and activity. Nat. Biotechnol. *38*, 883–891.
58. Xu, L., Liu, Y., and Han, R. (2019). BEAT: a Python program to quantify base editing from sanger sequencing. CRISPR J *2*, 223–229.
59. Newby, G.A., and Liu, D.R. (2021). In vivo somatic cell base editing and prime editing. Mol. Ther. *29*, 3107–3124.
60. Liang, P., Xie, X., Zhi, S., Sun, H., Zhang, X., Chen, Y., Chen, Y., Xiong, Y., Ma, W., Liu, D., et al. (2019). Genome-wide profiling of adenine base editor specificity by EndoV-seq. Nat. Commun. *10*, 67.
61. Bae, S., Park, J., and Kim, J.S. (2014). Cas-OFFinder: a fast and versatile algorithm that searches for potential off-target sites of Cas9 RNA-guided endonucleases. Bioinformatics *30*, 1473–1475.
62. Walton, R.T., Christie, K.A., Whittaker, M.N., and Kleinstiver, B.P. (2020). Unconstrained genome targeting with near-PAMless engineered CRISPR-Cas9 variants. Science *368*, 290–296.
63. Goemans, N.M., Tulinius, M., van den Akker, J.T., Burm, B.E., Ekhart, P.F., Heuvelmans, N., Holling, T., Janson, A.A., Platenburg, G.J., Sipkens, J.A., et al. (2011). Systemic administration of PRO051 in Duchenne's muscular dystrophy. N. Engl. J. Med. *364*, 1513–1522.
64. Mendell, J.R., Rodino-Klapac, L.R., Sahenk, Z., Roush, K., Bird, L., Lowes, L.P., Alfano, L., Gomez, A.M., Lewis, S., Kota, J., et al. (2013). Eteplirsen for the treatment of Duchenne muscular dystrophy. Ann. Neurol. *74*, 637–647.
65. Lee, H.K., Willi, M., Miller, S.M., Kim, S., Liu, C., Liu, D.R., and Hennighausen, L. (2018). Targeting fidelity of adenine and cytosine base editors in mouse embryos. Nat. Commun. *9*, 4804.
66. Haapaniemi, E., Botla, S., Persson, J., Schmierer, B., and Taipale, J. (2018). CRISPR-Cas9 genome editing induces a p53-mediated DNA damage response. Nat. Med. *24*, 927–930.
67. Ihry, R.J., Worringer, K.A., Salick, M.R., Frias, E., Ho, D., Theriault, K., Kommineni, S., Chen, J., Sondey, M., Ye, C., et al. (2018). p53 inhibits CRISPR-Cas9 engineering in human pluripotent stem cells. Nat. Med. *24*, 939–946.
68. Li, J., Wang, K., Zhang, Y., Qi, T., Yuan, J., Zhang, L., Qiu, H., Wang, J., Yang, H.T., Dai, Y., et al. (2021). Therapeutic exon skipping via a CRISPR-guided cytidine deaminase rescues dystrophic cardiomyopathy in vivo. Circulation *144*, 1760–1776.
69. Biendarra-Tiegs, S.M., Secreto, F.J., and Nelson, T.J. (2020). Addressing variability and heterogeneity of induced pluripotent stem cell-derived cardiomyocytes. Adv. Exp. Med. Biol. *1212*, 1–29.
70. Hoffman, E.P., Bronson, A., Levin, A.A., Takeda, S., Yokota, T., Baudy, A.R., and Connor, E.M. (2011). Restoring dystrophin expression in duchenne muscular dystrophy muscle progress in exon skipping and stop codon read through. Am. J. Pathol. *179*, 12–22.
71. Godfrey, C., Muses, S., McClorey, G., Wells, K.E., Coursindel, T., Terry, R.L., Betts, C., Hammond, S., O'Donovan, L., Hildyard, J., et al. (2015). How much dystrophin is enough: the physiological consequences of different levels of dystrophin in the mdx mouse. Hum. Mol. Genet. *24*, 4225–4237.
72. Kawaguchi, S., Soma, Y., Nakajima, K., Kanazawa, H., Tohyama, S., Tabei, R., Hirano, A., Handa, N., Yamada, Y., Okuda, S., et al. (2021). Intramyocardial transplantation of human iPS cell-derived cardiac spheroids improves cardiac function in heart failure animals. JACC. Basic Transl. Sci. *6*, 239–254.
73. Rojas, S.V., Kensah, G., Rotaermel, A., Baraki, H., Kutschka, I., Zweigerdt, R., Martin, U., Haverich, A., Gruh, I., and Martens, A. (2017). Transplantation of purified iPSC-derived cardiomyocytes in myocardial infarction. PLoS One *12*, e0173222.
74. Shiba, Y., Gomibuchi, T., Seto, T., Wada, Y., Ichimura, H., Tanaka, Y., Ogasawara, T., Okada, K., Shiba, N., Sakamoto, K., et al. (2016). Allogeneic transplantation of iPS cell-derived cardiomyocytes regenerates primate hearts. Nature *538*, 388–391.
75. Silver, S.E., Barrs, R.W., and Mei, Y. (2021). Transplantation of human pluripotent stem cell-derived cardiomyocytes for cardiac regenerative therapy. Front. Cardiovasc. Med. *8*, 707890.
76. Koblan, L.W., Doman, J.L., Wilson, C., Levy, J.M., Tay, T., Newby, G.A., Maianti, J.P., Raguram, A., and Liu, D.R. (2018). Improving cytidine and adenine base editors by expression optimization and ancestral reconstruction. Nat. Biotechnol. *36*, 843–846.
77. Wang, P., Xu, L., Gao, Y., and Han, R. (2020). BEON: a functional fluorescence reporter for quantification and enrichment of adenine base-editing activity. Mol. Ther. *28*, 1696–1705.